Supporting Information

PFAS Self Assembly and Adsorption Dynamics on Graphene: Molecular Insights into Chemical and Environmental Influences

Bradley Lamb, Boran Ma*

School of Polymer Science and Engineering, University of Southern Mississippi, 118 College Drive, Hattiesburg, MS 39406, USA.
* E-mail: boran.ma@usm.edu

The radius of gyration (R_g), fractal dimension (D_f), and asphericity (A_{sp}) results for long- and short-chain PFAS are presented in **Figures S1** and **S2**, respectively.

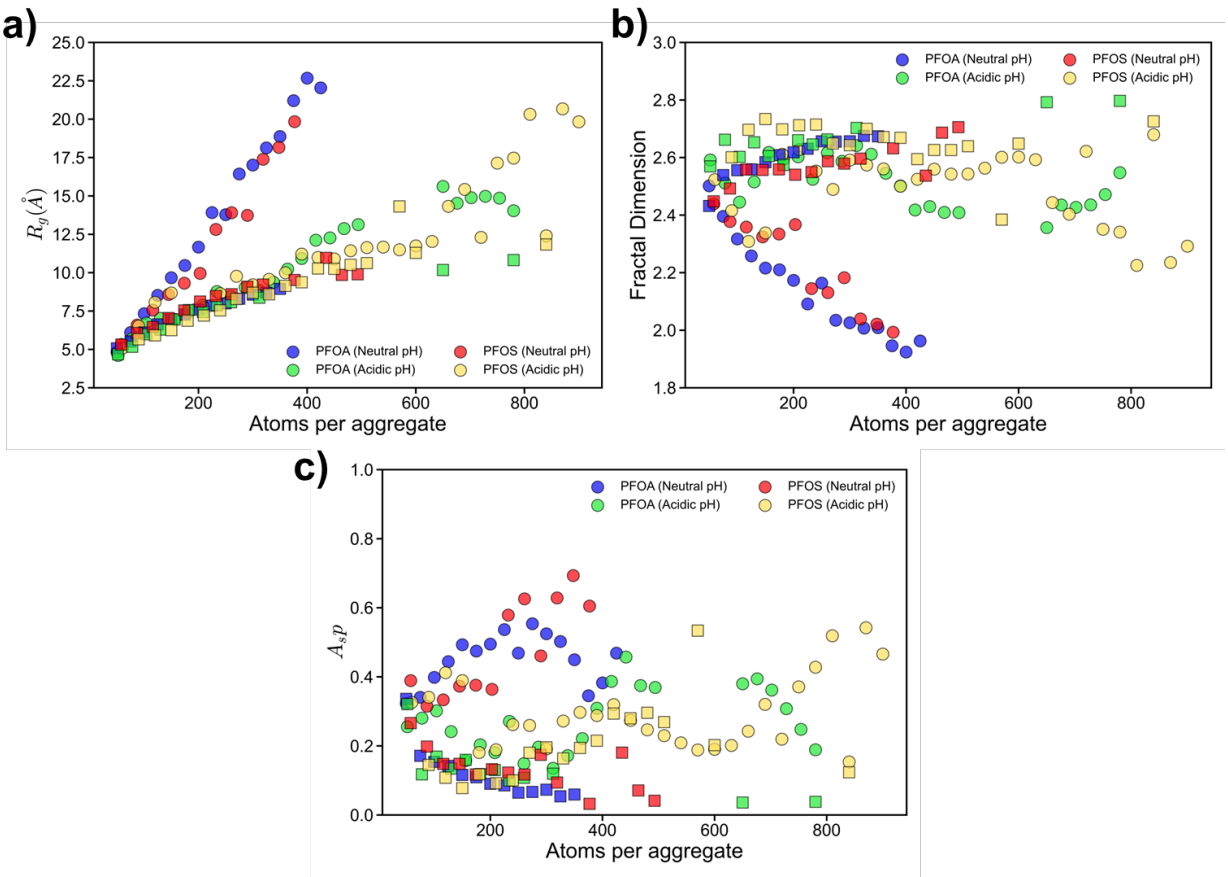

Figure S1. Long-chain PFAS aggregate data including a) radius of gyration, b) fractal dimension, and c) asphericity. Circles represent aggregates bound to the sorbent and squares represent aggregates in solution.

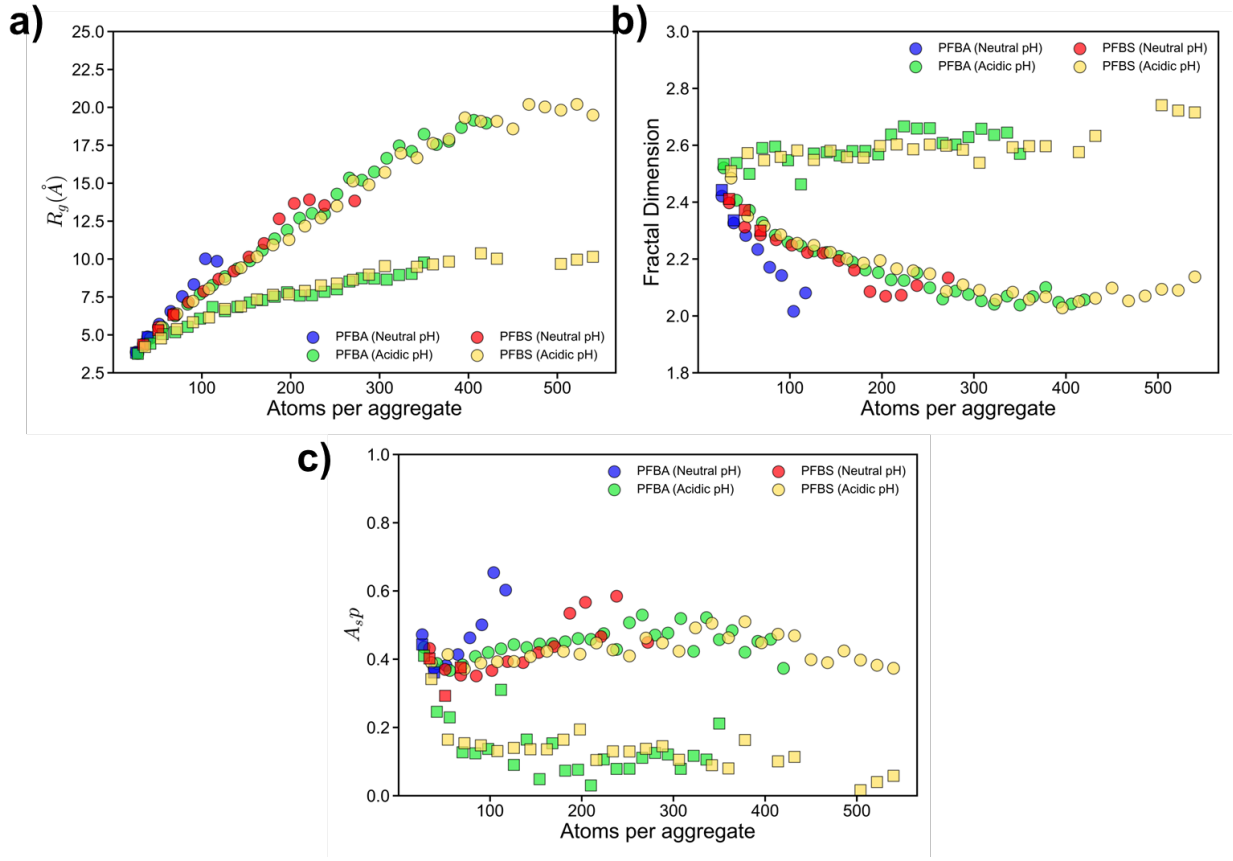

Figure S2. Short-chain PFAS aggregate data including a) radius of gyration, b) fractal dimension, and c) asphericity. Circles represent aggregates bound to the sorbent and squares represent aggregates in solution.

At acidic pH, aggregates of long-chain PFAS in solution exhibit similar trends to their bound counterparts in terms of R_g, D_f, and A_{sp}, **figure S1**. In both scenarios, the neutral headgroups enable tight packing of PFAS molecules, facilitating clustered aggregation through maximized hydrophobic interactions between their fluoroalkyl chains. However, bound aggregates tend to diffuse across the substrate, forming dual-layer structures. This behavior is reflected in their smaller D_f and higher A_{sp} values compared to aggregates in solution under acidic conditions.
In contrast, at neutral pH, the aggregation behaviors of long-chain PFAS differ significantly between the solution phase and those bound to the sorbent. In solution, headgroup repulsions drive the formation of micelle-like aggregates characterized by high D_f, low A_{sp}. Meanwhile, bound aggregates do not form multilayered structures. Instead, they adopt row-like arrangements with much lower D_f and higher A_{sp} values.
Interestingly, short-chain PFAS exhibit trends opposite to those observed for long-chain PFAS, **figure S2**. At neutral pH, short-chain PFAS do not form aggregates exceeding 100 atoms in solution. However, at acidic pH, they form much larger aggregates, exceeding 350 atoms for

PFBA and 500 atoms for PFBS. Additionally, at acidic pH, the solution-state aggregates display smaller R_g, along with larger D_f and A_{sp} values. This behavior arises from the high mobility of short-chain PFAS. In solution, the absence of headgroup repulsions allows short-chain PFAS to pack into large, spherical aggregates, as reflected by their high D_f (approximately 2.6) and low A_{sp} (around 0.1). Once bound to the sorbent, however, short-chain PFAS rapidly diffuse across the sorbent surface, forming two-dimensional row-like structures. This arrangement is characterized by a D_f value of approximately 2.0.

Top-down views of the adsorbed PFAS are shown in **Figures S3** and **S4**, depicting long- and short-chain PFAS, respectively.

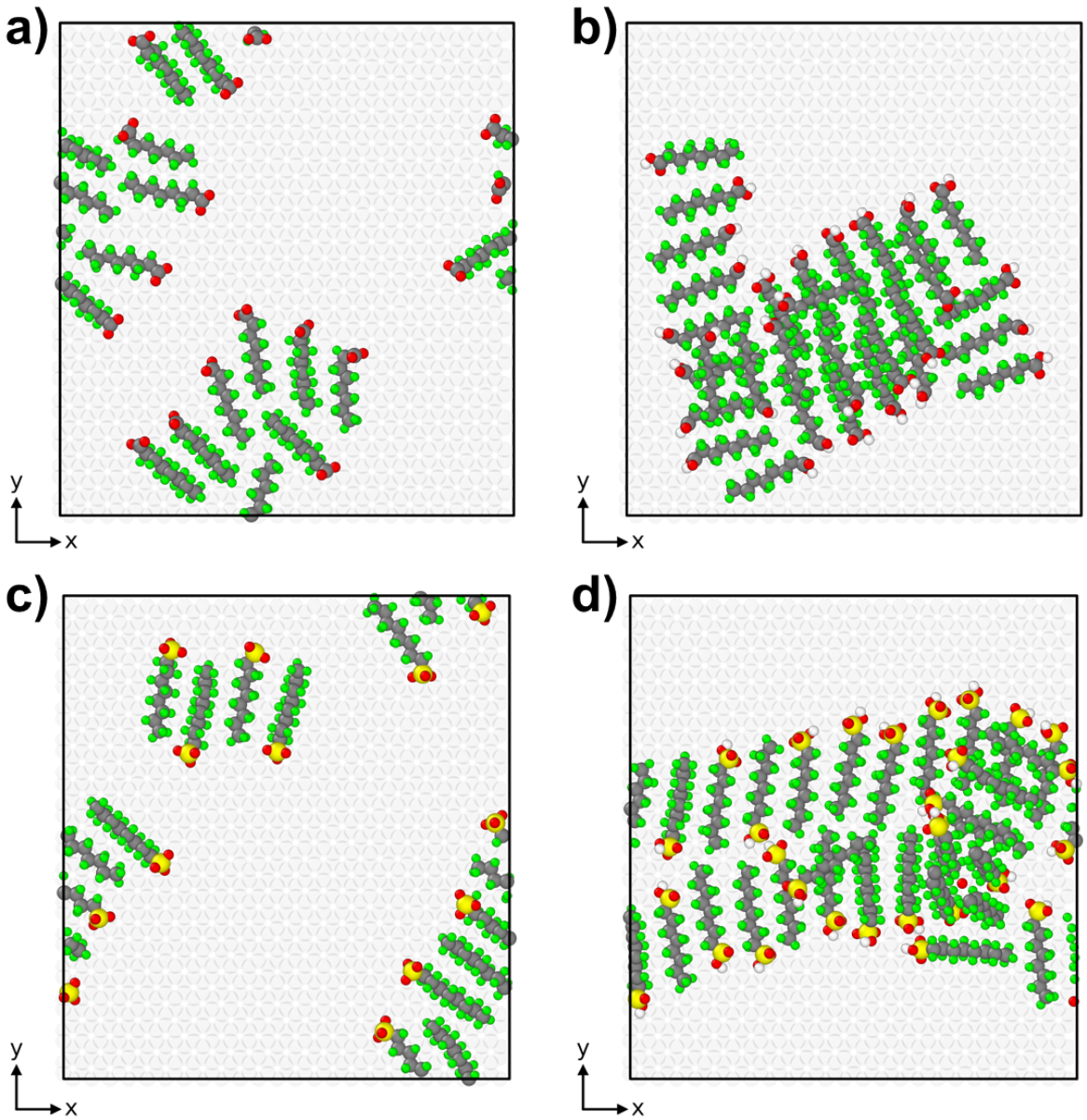

Figure S3. Top-down views of adsorbed a) PFOA at neutral pH and b) acidic pH, and c) PFOS at neutral pH and d) acidic pH.

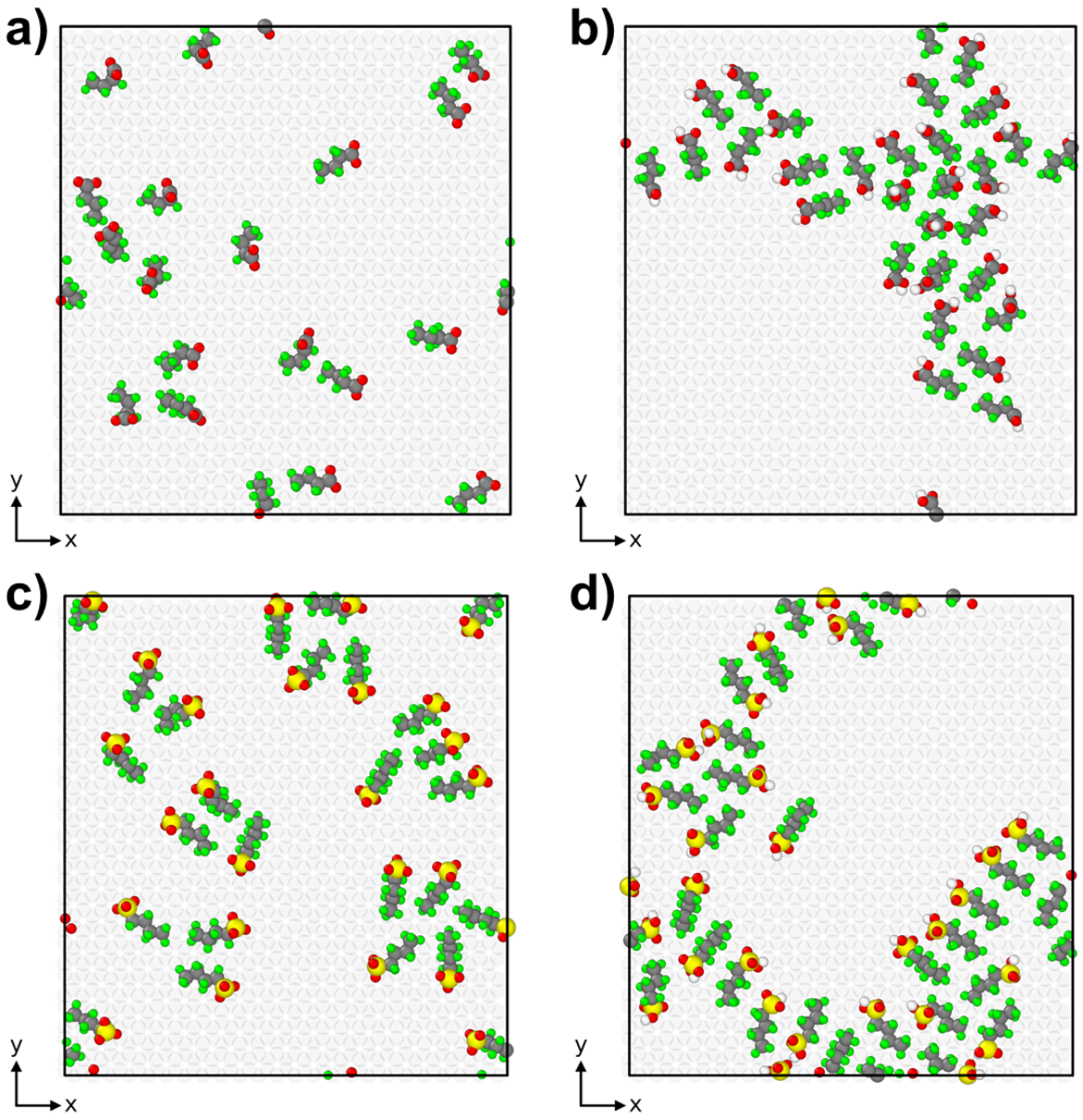

Figure S4. Top-down views of adsorbed a) PFBA at neutral pH and b) acidic pH, and c) PFBS at neutral pH and d) acidic pH.

Interactions between the sodium ions and the anionic PFAS headgroups were quantified with the radial distribution functions in **Figures S5** and **S6**, representing interactions of PFAS bound to the graphene and in solution respectively. Peaks maintained similar r distances for each PFAS, however, the intensity was stronger for short chain PFAS when bound to graphene (**figure S5**), and stronger for longer chain PFAS when in solution (**figure S6**). This is likely due to the higher adsorption angle for short chain PFAS, resulting in stronger interactions with sodium ions in solution. Whereas in solution, the longer chain PFAS form ordered aggregates in which the sodium ions strongly orient around relative to the dispersed short chain PFAS.

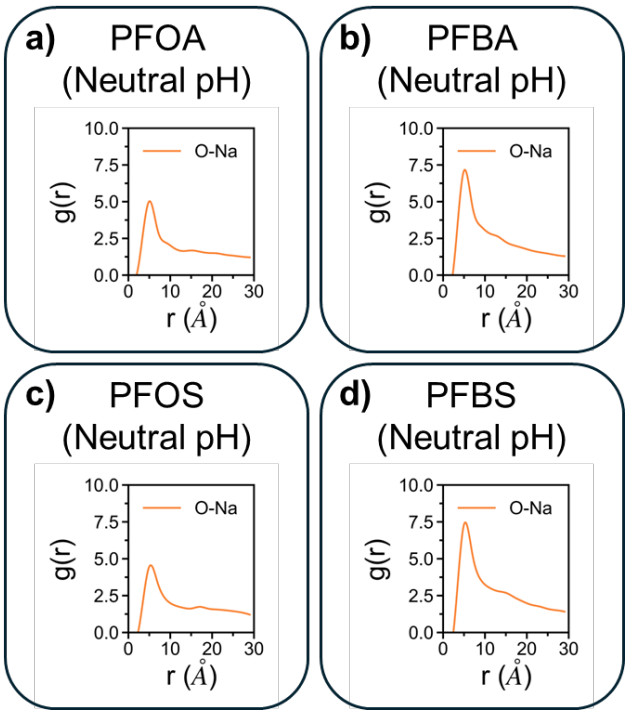

Figure S5. Radial distribution functions for PFAS anionic headgroups and sodium ions for **a)** PFOA, **b)** PFBA, **c)** PFOS, and **d)** PFBS at neutral pH, adsorbed to graphene.

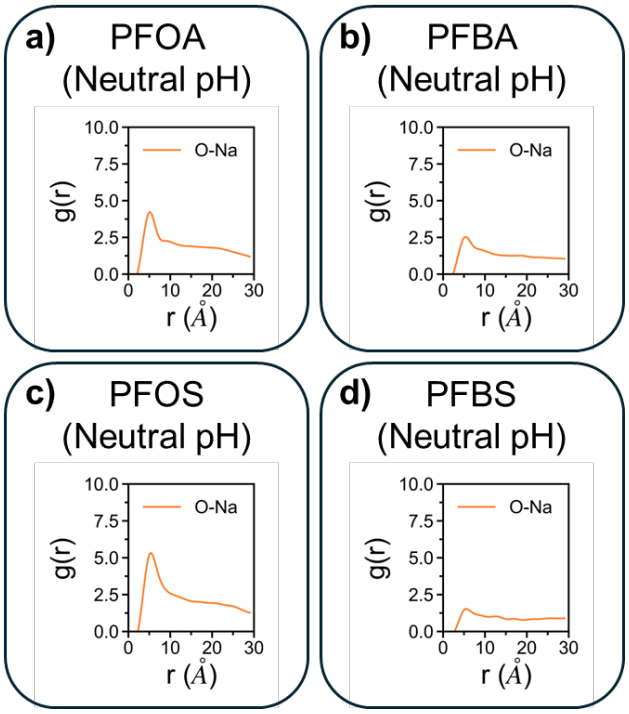

Figure S6. Radial distribution functions for PFAS anionic headgroups and sodium ions for **a)** PFOA, **b)** PFBA, **c)** PFOS, and **d)** PFBS at neutral pH, in solution.

Validation of the equilibration protocol used in this study was performed by applying the protocol used in this study on a system of water and PFAS, while the same system was equilibrated using an NPT based approach. Both methods produced consistent results, with volume, kinetic energy, and potential energy being within 1% of each other. The resulting volume and energy plots are displayed below in **Figure S7**, additionally showing the system is well equilibrated within 5ns as the values oscillate about a constant value for the duration.

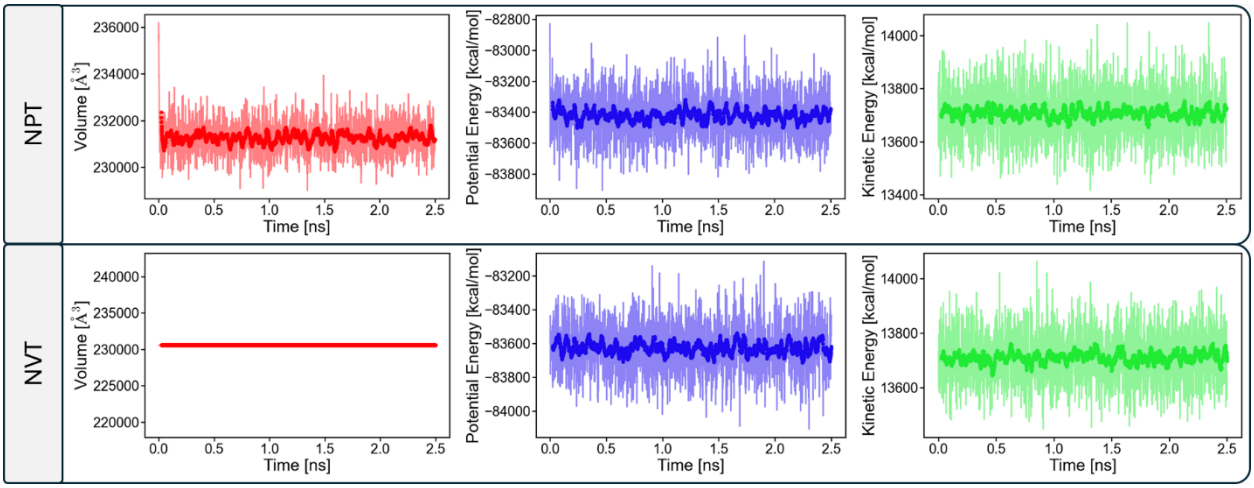

Figure S7. Summary of the volume and energy of the two equilibration methods, NPT and NVT, after resizing. Individual data points are made semi-transparent while the moving average is opaque for clarity.

The non-bonded forcefield parameters for the PFAS studied are summarized in T**ables S1 – S8**. Additionally, the molecule ids from the ATB database for the respective PFAS are as follows, respectively: 250937, 1394233, 1670948, 1394612, 517853, 1756668, 276072, 962972.

Table S1. Non-bonded forcefield parameters for PFOA at neutral pH, atoms reported as they are described by the GROMOS 54A7 forcefield.

Molecule	Atom	q (e)	σ (Å)	ϵ (kcal/mol)
PFOA (neutral pH)	C	0.126	6.30E-02	3.58E+00
	C	0.122		
	C	0.104		
	CPos	0.384	2.45E-01	2.81E+00
	CPos	0.197		
	CPos	0.186		
	CPos	0.273		
	CPos	0.653		
	F	-0.111	1.09E-01	2.94E+00
	F	-0.111		
	F	-0.111		
	F	-0.085		
	F	-0.085		
	F	-0.083		
	F	-0.083		
	F	-0.090		
	F	-0.090		
	F	-0.096		
	F	-0.096		
	F	-0.109		
	F	-0.109		
	F	-0.190		
	F	-0.190		
	NA+	1.000	5.09E-03	3.12E+00
	OM	-0.703	4.12E-01	2.63E+00
	OM	-0.703		

Table S2. Non-bonded forcefield parameters for PFOA at acidic pH, atoms reported as they are described by the GROMOS 54A7 forcefield.

Molecule	Atom	q (e)	σ (Å)	ϵ (kcal/mol)
PFOA (acidic pH)	C	0.133	6.30E-02	3.58E+00
	C	0.098		
	C	0.097		
	CPos	0.392	2.45E-01	2.81E+00
	CPos	0.223		
	CPos	0.162		
	CPos	0.289		
	CPos	0.665		
	F	-0.112	1.09E-01	2.94E+00
	F	-0.112		
	F	-0.112		
	F	-0.085		
	F	-0.085		
	F	-0.075		
	F	-0.075		
	F	-0.087		
	F	-0.087		
	F	-0.083		
	F	-0.083		
	F	-0.094		
	F	-0.094		
	F	-0.141		
	F	-0.141		
	HS14	0.482	0.00E+00	0.00E+00
	OA	-0.566	2.03E-01	2.95E+00
	OEOpt	-0.509	1.19E-01	3.40E+00

Table S3. Non-bonded forcefield parameters for PFBA at neutral pH, atoms reported as they are described by the GROMOS 54A7 forcefield.

Molecule	Atom	q (e)	σ (Å)	ϵ (kcal/mol)
PFBA (neutral pH)	CPos	0.425	2.45E-01	2.81E+00
	CPos	0.267		
	CPos	0.199		
	CPos	0.647		
	F	-0.150	1.09E-01	2.94E+00
	F	-0.150		
	F	-0.150		
	F	-0.161		
	F	-0.161		
	F	-0.186		
	F	-0.186		
	NA+	1.000	5.09E-03	3.12E+00
	OM	-0.697	4.12E-01	2.63E+00
	OM	-0.697		

Table S4. Non-bonded forcefield parameters for PFBA at acidic pH, atoms reported as they are described by the GROMOS 54A7 forcefield.

Molecule	Atom	q (e)	σ (Å)	ϵ (kcal/mol)
PFBA (acidic pH)	C	0.057	6.30E-02	3.58E+00
	CPos	0.417	2.45E-01	2.81E+00
	CPos	0.245		
	CPos	0.666		
	F	-0.119	1.09E-01	2.94E+00
	F	-0.119		
	F	-0.119		
	F	-0.087		
	F	-0.087		
	F	-0.136		
	F	-0.136		
	HS14	0.479	0.00E+00	0.00E+00
	OA	-0.56	2.03E-01	2.95E+00
	OEOpt	-0.501	1.19E-01	3.40E+00

Table S5. Non-bonded forcefield parameters for PFOS at neutral pH, atoms reported as they are described by the GROMOS 54A7 forcefield.

Molecule	Atom	q (e)	σ (Å)	ϵ (kcal/mol)
PFOS (neutral pH)	C	0.128	6.30E-02	3.58E+00
	C	0.139		
	C	0.069		
	CPos	0.387	2.45E-01	2.81E+00
	CPos	0.159		
	CPos	0.205		
	CPos	0.190		
	CPos	0.201		
	F	-0.112	1.09E-01	2.94E+00
	F	-0.112		
	F	-0.112		
	F	-0.087		
	F	-0.087		
	F	-0.090		
	F	-0.090		
	F	-0.093		
	F	-0.093		
	F	-0.086		
	F	-0.086		
	F	-0.093		
	F	-0.093		
	F	-0.099		
	F	-0.099		
	F	-0.097		
	F	-0.097		
	NA+	1.000	5.09E-03	3.12E+00
	OM	-0.560	4.12E-01	2.63E+00
	OM	-0.560		
	OM	-0.560		
	SDmso	0.828	3.10E-01	3.56E+00

Table S6. Non-bonded forcefield parameters for PFOS at acidic pH, atoms reported as they are described by the GROMOS 54A7 forcefield.

Molecule	Atom	q (e)	σ (Å)	ϵ (kcal/mol)
PFOS (acidic pH)	C	0.117	6.30E-02	3.58E+00
	C	0.15		
	C	0.138		
	C	0.021		
	CPos	0.393	2.45E-01	2.81E+00
	CPos	0.201		
	CPos	0.180		
	CPos	0.211		
	F	-0.112	1.09E-01	2.94E+00
	F	-0.112		
	F	-0.112		
	F	-0.083		
	F	-0.083		
	F	-0.085		
	F	-0.085		
	F	-0.088		
	F	-0.088		
	F	-0.078		
	F	-0.078		
	F	-0.079		
	F	-0.079		
	F	-0.086		
	F	-0.086		
	F	-0.043		
	F	-0.043		
	HS14	0.481	0.00E+00	0.00E+00
	OEOpt	-0.473	1.19E-01	3.40E+00
	OM	-0.415	4.12E-01	2.63E+00
	OM	-0.415		
	SDmso	0.831	3.10E-01	3.56E+00

Table S7. Non-bonded forcefield parameters for PFBS at neutral pH, atoms reported as they are described by the GROMOS 54A7 forcefield.

Molecule	Atom	q (e)	σ (Å)	ϵ (kcal/mol)
PFBS (neutral pH)	C	0.120	6.30E-02	3.58E+00
	C	0.095		
	CPos	0.382	2.45E-01	2.81E+00
	CPos	0.176		
	F	-0.115	0.109	2.94
	F	-0.115		
	F	-0.115		
	F	-0.088		
	F	-0.088		
	F	-0.099		
	F	-0.099		
	F	-0.098		
	F	-0.098		
	NA+	1.000	5.09E-03	3.12E+00
	OM	-0.558	0.4122	2.6258
	OM	-0.558		
	OM	-0.558		
	SDmso	0.816	3.10E-01	3.56E+00

Table S8. Non-bonded forcefield parameters for PFBS at acidic pH, atoms reported as they are described by the GROMOS 54A7 forcefield.

Molecule	Atom	q (e)	σ (Å)	ϵ (kcal/mol)
PFBS (acidic pH)	C	0.142	6.30E-02	3.58E+00
	C	0.098		
	CPos	0.359	2.45E-01	2.81E+00
	CPos	0.151		
	F	-0.104	0.109	2.94
	F	-0.104		
	F	-0.104		
	F	-0.080		
	F	-0.080		
	F	-0.082		
	F	-0.082		
	F	-0.056		
	F	-0.056		
	HS14	0.477	0.00E+00	0.00E+00
	OEOpt	-0.478	1.19E-01	3.40E+00

	OM	-0.421	4.12E-01	2.63E+00
	OM	-0.421		
	SDmso	0.841	3.10E-01	3.56E+00